The Optimal Swing-Leg Retraction Rate for Running

J.G.Daniël Karssen, Matt Haberland, Martijn Wisse, and Sangbae Kim

***Abstract*— Swing-leg retraction was introduced as a way to improve the stability and disturbance rejection of running robots. It was also suggested that the reduced foot speed due to swing-leg retraction can help reduce impact energy losses, decrease peak forces, and minimize foot slipping. However, the extent to which swing-leg retraction rate influences all these benefits was unknown. In this paper, we present a study on the effect of swing-leg retraction rate on these benefits. The results of this study show that swing-leg retraction can indeed improve the performance of running robots in all of the suggested areas. However, the results also show that, for moderate and high running speeds, the optimal retraction rate for maximal disturbance rejection and stability is different from the optimal retraction rate for minimal impact losses, peak forces, and foot slipping. This discrepancy indicates an inherent tradeoff to consider when selecting the retraction rate for a robot control system: in general, retraction rate can be optimized for better stability and disturbance rejection or for more favorable efficiency, impact forces, and footing stability, but not all simultaneously. Furthermore, this tradeoff becomes more severe as running speed increases.**

I. INTRODUCTION

There has been great interest in developing dynamic legged robots for decades. Recently, legged robots began to demonstrate advantages over conventional wheeled and tracked vehicles over highly rough terrain [1].

One of the most effective ways used to control the motion of dynamic legged robots is to adjust the angle at which the legs make contact with the ground, the so-called angle-of-attack. This is implemented by controllers like Raibert's foot placement strategy [2], constant angle-of-attack control [3], [4], and passive foot placement [5]. They show that angle-of-attack significantly affects the dynamics of running robots. However, leg speed with respect to the ground at the moment of foot contact may also be very important to running robot performance.

Animals and humans seem to use a leg speed control strategy called swing-leg retraction [6]: they rotate the front leg backward toward the end of the flight phase. Seyfarth et al. [7] showed that swing-leg retraction can increase the stability of the running motion. For walking, Wisse et al. [8] and Hobbelen et al. [9] showed that swing-leg retraction can also increase the disturbance rejection.

J.G.D. Karssen and M. Wisse are funded by the Dutch Technology Foundation STW and are with the Delft Biorobotics Laboratory, Department of BioMechanical Engineering, Faculty of Mechanical Engineering, Delft University of Technology, 2628 CD, Delft, The Netherlands j.g.d.karssen@tudelft.nl.

M. Haberland and S. Kim are funded by the Defense Advanced Research Project Agency and are with the Biomimetic Robotics Laboratory, Department of Mechanical Engineering, Massachusetts Institute of Technology, 77 Massachusetts Avenue, Cambridge, Massachusetts, USA mdhaber@mit.edu.

Swing-leg retraction is also believed to offer advantages other than improved stability and disturbance rejection. By reducing the relative speed between the foot and the ground at the moment of contact [2], [10], swing-leg retraction can reduce impact losses, the chance of slipping, and damaging impact forces.

The hypothesized benefits of swing-leg retraction are well known, however the optimal swing-leg retraction rate is unknown. Also, is it unknown how the optimal swing-leg retraction rate depends on system parameters, like leg stiffness and horizontal velocity. Knowledge of the optimal swing-leg retraction rate is crucial for implementing swing-leg retraction on a running robot, because an excessive retraction rate can adversely affect running performance. The goal of this paper is to provide methods and simulation results that determine the retraction rates that result in the optimal running performance.

The remainder of this paper is organized as follows. Section II describes the model used in this study. In Section III the effect of the swing-leg retraction rate on the disturbance rejection of this model is discussed. Next the effect of the swing-leg retraction rate on the other advantages of swing-leg retraction, like the reduced impact losses, are discussed in Section IV. The paper ends with a discussion in Section V and the conclusions in Section VI.

II. SIMULATION MODEL

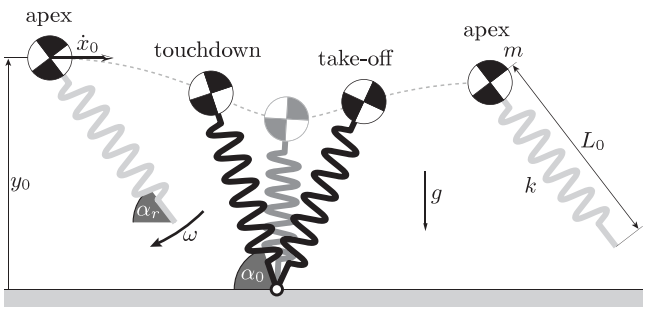

Fig. 1. A simple running model with swing-leg retraction. The model consists of a point mass body and a massless spring leg. At the apex the leg is at an angle α_r with respect to the ground and starts rotating with a rate ω. The leg angle at touchdown α_0 depends on the time between apex and touchdown.

For this study, we use the simple spring-mass model that Blickhan introduced for analyzing running motions [3]. This model consists of a point mass on a massless spring (see figure 1). Some refer to it as the spring loaded inverted pendulum (SLIP) model, because the spring behaves like an inverted pendulum during the stance phase [11]. The simplicity of this model makes it desirable for studying fundamental

TABLE I

MODEL PARAMETER VALUES

Parameter	Symbol	Value	Unit
Mass	m	80	[kg]
Gravitational constant	g	9.81	[m/s^2]
Nominal leg length	l_0	1.0	[m]
Leg stiffness	k	20000	[N/m]
Angle-of-attack	α_0	66.44	[°]
Apex height	y_0	1.0	[m]
Horizontal velocity	$\dot{x}_0$	5.0	[m/s]

properties of running without interfering complexities. Note that this model does not include collision losses, impact forces, or the possibility of slipping due to the massless leg. However in Section IV, we introduce leg mass and inertia to investigate the effect swing-leg retraction on the collision losses, impact forces, and the likelihood of slipping.

The running motion of this model has two distinct phases, a stance phase and a flight phase. During the stance phase, the motion is given by:

$$m \begin{bmatrix} \ddot{x} \\ \ddot{y} \end{bmatrix} = \begin{bmatrix} -\cos\alpha \\ \sin\alpha \end{bmatrix} F_s + \begin{bmatrix} 0 \\ -mg \end{bmatrix}, \tag{1}$$

where α is the angle that the leg makes with the ground and F_s is the spring force. The leg spring is a linear spring, so the spring force is proportional to the leg compression ΔL,

$$F_s = k\Delta L, \tag{2}$$

where k is the leg stiffness. The stance phase ends and the flight phase begins at take-off, when the spring leg is at its rest length L_0. During the flight phase, the point mass follows a ballistic trajectory, as the spring does not apply any force. The swing leg assumes an angle of α_r with respect to the ground at apex and begins rotating backward with retraction rate ω. The flight phase ends and the stance phase begins when the leg touches down. The leg angle at touchdown depends on the time between apex and touchdown.

For the purpose of analysis, the start of a step is defined as the apex of the flight phase. At apex, the vertical velocity is zero and the state of the model is described by two initial conditions, apex height y_0 and horizontal velocity $\dot{x}_0$. The initial conditions of a step can be mapped on the initial conditions of the next step with the stride function S.

$$\mathbf{v}_{n+1} = S(\mathbf{v}_n) \qquad \text{with } \mathbf{v} = \begin{bmatrix} y_0 \\ \dot{x}_0 \end{bmatrix} \tag{3}$$

The stride function can have fixed points, where the initial conditions result in the same initial conditions after a single step.

$$\mathbf{v}^* = S(\mathbf{v}^*) \tag{4}$$

If the model is started in a fixed point, it will undergo a periodic motion. This repeated motion is called a limit cycle.

Throughout this study, we use humanlike values for the model parameters, unless otherwise noted. These humanlike values are taken from Seyfarth et al. [12] and are shown in table I. The angle of the leg at apex α_r is set depending on the retraction rate ω such that the leg angle at touchdown α_0 is 66.44°, which is the value required for limit cycle running at the chosen apex height and apex horizontal velocity. However, even though the leg angle at apex α_r remains constant for a given ω, the leg angle at touchdown α_0 changes if the model is disturbed from its limit cycle.

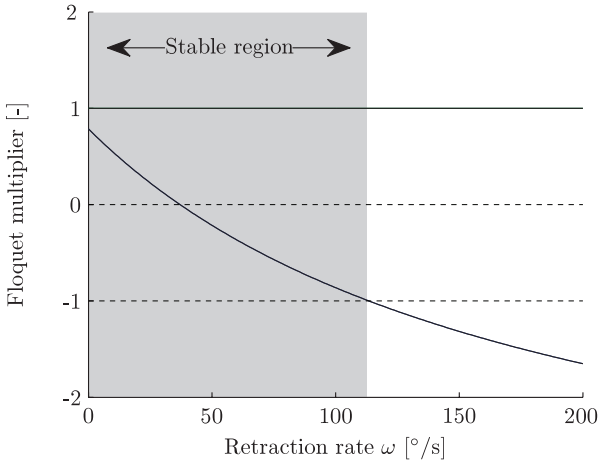

Fig. 2. The two Floquet multipliers on the linearized step-to-step map as functions of the retraction rate. One of the Floquet multipliers is always one, due to the energy conservative nature of the model. The other Floquet multiplier decreases with an increasing retraction rate. Beyond a retraction rate of 113°/s the magnitude of one of Floquet multipliers is larger than one, indicating that the model is unstable at these retraction rates.

III. DISTURBANCE REJECTION

Swing-leg retraction is introduced as a simple control strategy to increase the disturbance rejection of running systems. In this section, we investigate how the disturbance rejection is influenced by the swing-leg retraction rate. First, we analyze how the retraction rate influences the model's response to very small disturbances. Next, we look at the largest single disturbance the model can handle without falling. At the end of this section, we investigate how well the model with swing-leg retraction can accommodate multiple disturbances in succession.

A. Stability

The stability of a running model can be assessed by looking at the stability of the linearized step-to-step behavior [5], [7], [9]. This stability is expressed in terms of Floquet multipliers, which are the eigenvalues of the linearized step-to-step map A.

$$\Delta\mathbf{v}_{n+1} = A\Delta\mathbf{v}_n \qquad \text{with } \Delta\mathbf{v}_n = \mathbf{v}_n - \mathbf{v}^* \tag{5}$$

The Floquet multipliers indicate how fast the model converges back to the limit cycle after a small deviation from the limit cycle. A system is stable if the magnitude of all Floquet multipliers is less than or equal to one. Our running model has two Floquet multipliers as it has two initial condition variables.

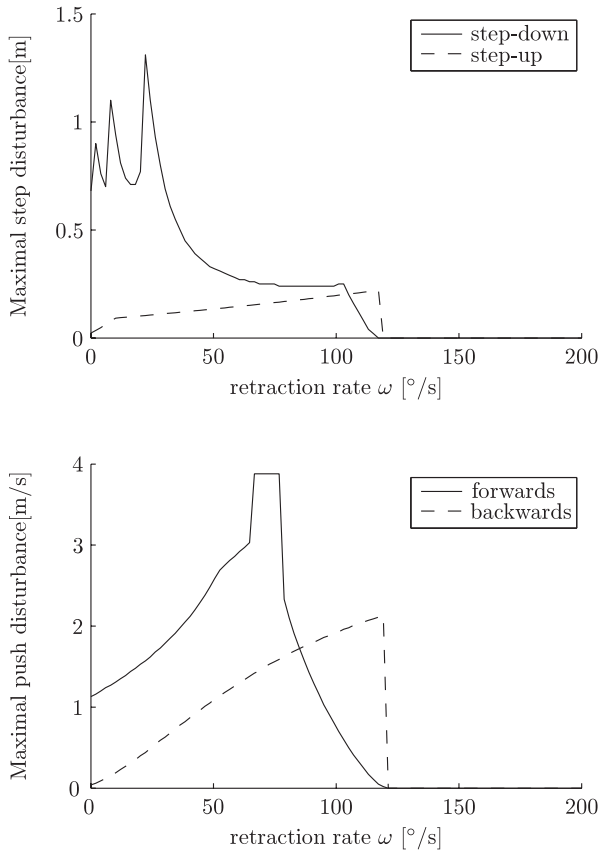

Fig. 3. The maximal single disturbance after which the model can run a 100 steps without falling as function of the retraction rate for four kind of disturbances.

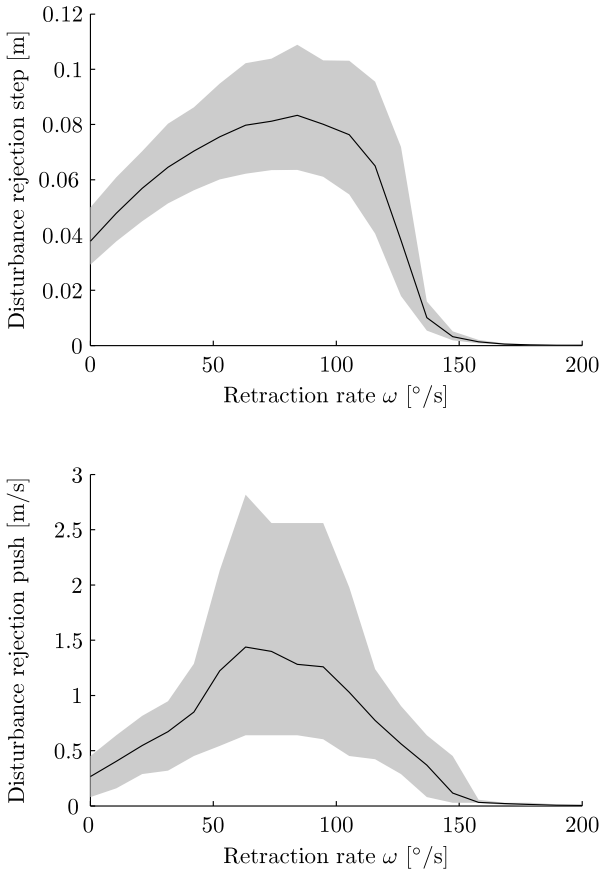

Fig. 4. The maximal random disturbance as function of the retraction rate for step and push disturbances. The black line is the average of a 100 trials and the gray area indicates the range where 95% of the trials lie.

Figure 2 shows how the two Floquet multipliers vary across a range of swing-leg retraction rates. Due to the energy conservative nature of the model, one of the Floquet multipliers is always one: disturbances to energy level persist. Neither swing leg retraction nor any other angle-of-attack controller can affect this. The other Floquet multiplier decreases with increasing retraction rate. At a retraction rate of 37°/s this Floquet multiplier is zero, indicating that the stability of the model is optimal at this rate. The zero Floquet multiplier causes the model to return to the original limit cycle within a single step of small, energy-neutral disturbances. For higher retraction rates the model becomes less stable and beyond a retraction rate of 113°/s the model is unstable. This indicates that retraction rates higher than 113°/s are not useful when swing-leg retraction is the complete control strategy, as even the smallest disturbance will cause the model to deviate from its limit cycle.

B. Single disturbance

The Floquet multipliers only indicate whether the model is stable with respect to small disturbances. They do not predict how the model will respond to large disturbances because they assume a linear disturbance response even though the model's disturbance response is actually non-linear. To investigate the response to realistic disturbances, we determine the maximal disturbance from which the model can recover for a range of retraction rates. Two disturbance types are used, a terrain step and a push. Both disturbances are implemented as a change in the initial conditions. The step disturbance results in a change of the apex height,

$$y_0 = y_0^* + d_{step}, \tag{6}$$
$$\dot{x}_0 = \dot{x}_0^*, \tag{7}$$

and the push disturbance in a change of the horizontal velocity,

$$y_0 = y_0^*, \tag{8}$$
$$\dot{x}_0 = \dot{x}_0^* + d_{push}. \tag{9}$$

Figure 3 shows the maximal disturbance as a function of the retraction rate for both disturbances in the positive and negative directions. As predicted by the Floquet multipliers, all four graphs show that retraction rates above 113°/s do not permit recovery from disturbances. However, there are no other shared trends among the graphs. The maximal disturbance does not clearly indicate a retraction rate for optimal disturbance rejection. This is partly due to the fact that the maximal disturbance is sometimes determined by artifacts of the model. For example, the maximal step-up

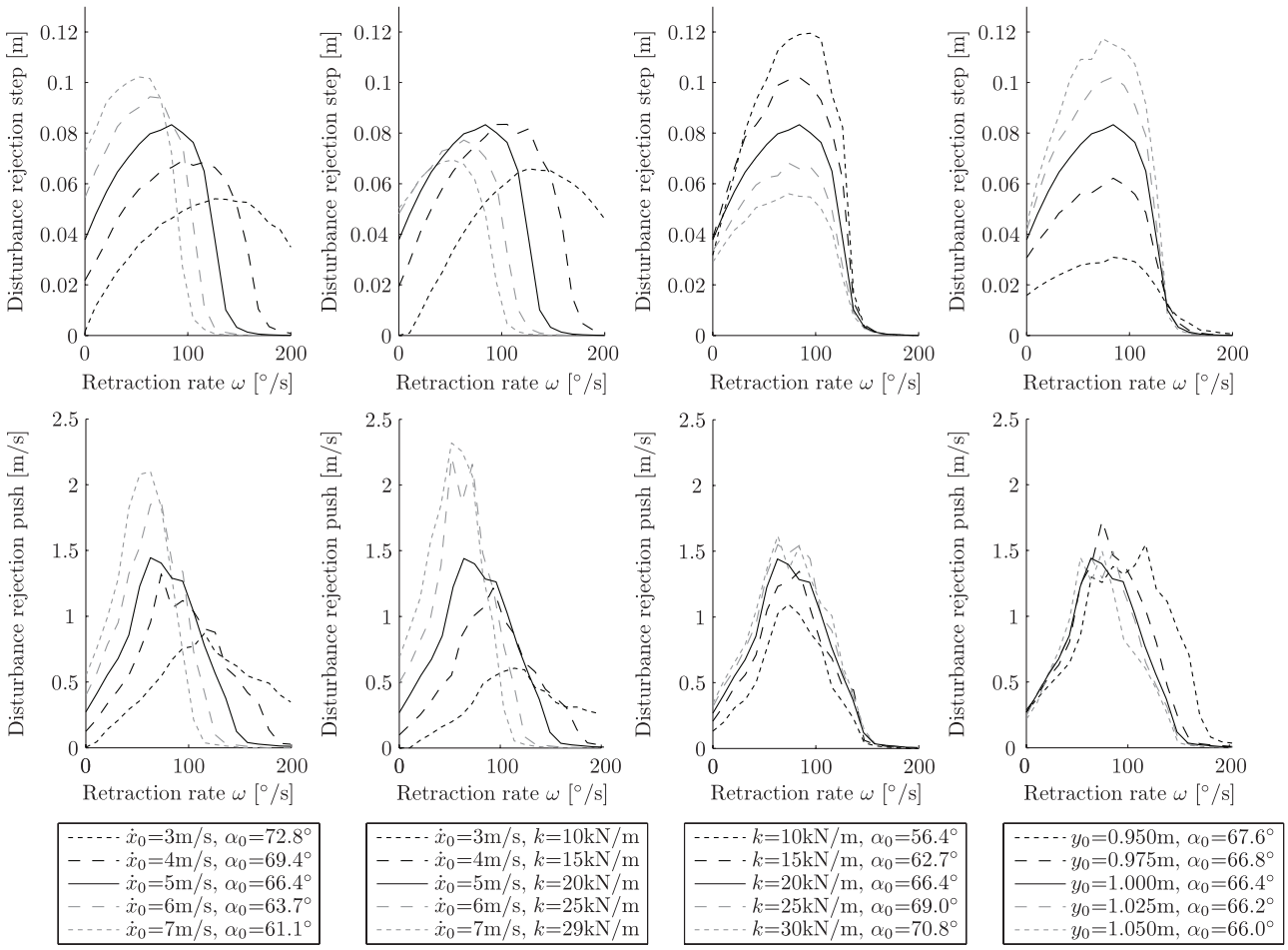

Fig. 5. The effect of parameter variations on the relationship between disturbance rejection and retraction rate. The top row shows the disturbance rejection for a step disturbance and the bottom row for a push disturbance. Each column shows one parameter pair variation. Only parameter pair variations that include a change in the horizontal velocity (two left columns) affect the retraction rate for which the disturbance rejection is maximal.

disturbance is, for a large range of retraction rates, equal to the amount of ground clearance at the apex.

C. Multiple disturbances

The maximal disturbance tests did not give a clear indication on which retraction rate is optimal. To gain insight about the optimal retraction rate for disturbance rejection, we consider how the model reacts to multiple disturbances in succession. For this we use the disturbance rejection measure as defined by Hobbelen et al. [13]. They quantified the disturbance rejection as the maximal variance of a Gaussian white noise sequence that, when applied as successive step or push disturbances, causes the model to fall exactly four times in an 80 step trial. This disturbance rejection measure is noisy, due to the random disturbances it uses to test the disturbance rejection. To decrease the noise, the measure is calculated 100 times and averaged. Note that this measure is very computationally intensive; it takes about one hour to calculate the disturbance rejection for one parameter set. Therefore, the disturbance rejection is determined for a limited number of retraction rates in the range of interest.

Figure 4 gives the disturbance rejection for a range of retraction rates for step and push disturbances. For both types of disturbances, the disturbance rejection is improved by swing-leg retraction. The disturbance rejection is optimal at a retraction rate of about 85°/s for the step disturbances and about 70°/s for the push disturbances. Around these optimal retraction rates the disturbance rejection is relatively constant for a range of about 20°/s, so it is possible to select a retraction rate such that the disturbance rejection is high for both step and push disturbances.

It should be noted that the retraction rates for the optimal disturbance rejection are not close to the retraction rate for the optimal stability determined in Section III-A. This shows that stability and disturbance rejection are not interchangeable quantities. This agrees with the results of Hobbelen et al. [13], who showed similar discrepancies between stability and disturbance rejection in walking models.

D. Parameter variations

We showed the relation between the retraction rate and the disturbance rejection for a single parameter set. In this section, we test the effect of parameter variations. There are 7 fixed parameters in the model used in this study (see table I). Three of these parameters, mass, gravitational constant and leg length, can be used to normalize the system and will

therefore have only a trivial scaling effect on the relation between disturbance rejection and retraction rate. This leaves four parameters to vary: leg stiffness k, angle-of-attack α_0, apex height y_0 and horizontal velocity $\dot{x}_0$. It is not possible to vary these parameters independently, because the model only has limit cycles for certain combinations of parameter values. Therefore, we vary these parameters in pairs, setting one parameter to a desired value and adjusting the other parameter such that there is a limit cycle.

The results of the parameter variations are shown in figure 5. All the parameter variations have an effect on the disturbance rejection. However, in the context of this paper not all the changes in the disturbance rejection are interesting, because we are only interested in how optimal retraction rates, as measured by the maxima of the disturbance rejection curves, change due to parameter variations. Only parameter variations that include varying the horizontal velocity have an effect on the optimal retraction rate. Based on this we can conclude that the optimal retraction rate is only dependent on the horizontal velocity. The swing-leg retraction rate for maximal disturbance rejection decreases with increasing horizontal velocity. For a horizontal velocity of 3 m/s the optimal retraction is about 130°/s and this decreases to 50°/s for a horizontal velocity of 7 m/s.

IV. OTHER BENEFITS

In the previous section, we showed how the disturbance rejection is affected by the retraction rate. In this section, we look how the other benefits of swing-leg retraction are affected by the retraction rate. There are three benefits of swing-leg retraction besides improved disturbance rejection: reduced impact losses, reduced chance of slipping, and a reduction of damaging impact forces. These three benefits are all due to the fact that swing-leg retraction reduces the relative speed of the foot with respect to the ground at the moment of touchdown. In this section, we first discuss the effect of the retraction rate on the relative foot speed. Next, we discuss how the relative foot speed relates to the three benefits.

A. Foot speed

The speed of the foot can be expressed in multiple ways. For the discussion in this section, the following speeds are important: the absolute v_{abs}, horizontal v_x, vertical v_y, tangential v_t, and axial v_a speed (see figure 6 for definitions). Swing-leg retraction increases the vertical speed and decreases both the horizontal and tangential speed. The absolute speed decreases with swing-leg retraction for low retraction rates and increases again for higher retraction rates. The minimum absolute speed is found at the retraction rate for which the tangential speed is zero. At this retraction rate, the absolute speed equals the axial velocity, which is not affected by swing-leg retraction. Note that this retraction rate is lower than the retraction rate for which the horizontal speed is zero, which is known as ground speed matching.

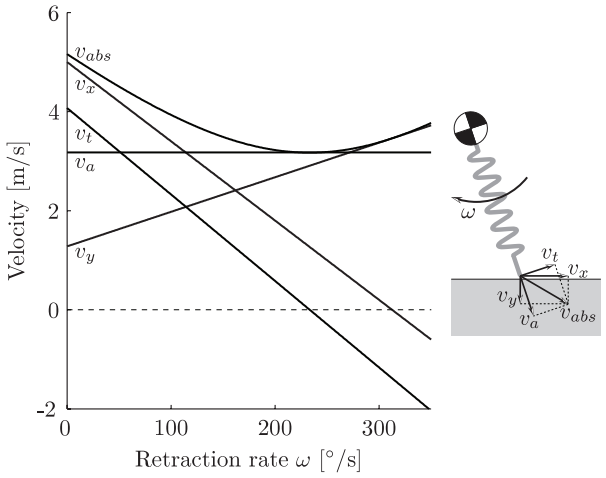

Fig. 6. The effect of swing-leg retraction on the speed of the foot just before contact. The absolute, horizontal, vertical, tangential, and axial speeds are shown. The insert figure shows how these speeds are defined. The angle-of-attack, leg length, apex height and horizontal apex velocity used this graph are given in table I.

B. Impact losses

The SLIP model used in this study does not have impact losses, because its leg has no inertia or unsprung foot mass. However, we can reason on how the impact losses of a model with leg inertia and foot mass would be affected by the speed of the foot at touchdown. For this we assume that the leg consists of distributed mass m with inertia J_{leg}, which is connected to a foot with point mass m_{foot} by a massless spring. We also assume that the impact is an instantaneous collision and that body parts, other than the leg that touches down, have no effect on the impact losses. The energy loss due to the impact of the foot mass $E_{loss,foot}$ is a function of the absolute foot speed v_{abs} and the foot mass m_{foot},

$$E_{loss,foot} = 1/2 m_{foot} v_{abs}^2. \tag{10}$$

The energy loss due to the leg inertia $E_{loss,leg}$ depends on the tangential speed v_t and the mass properties of the leg,

$$E_{loss,leg} = \frac{J_{leg} m}{2(mL_0^2 + J_{leg})} v_t^2. \tag{11}$$

The total energy loss $E_{loss,foot} + E_{loss,leg}$ is minimal if both the tangential and the absolute speed are minimal in magnitude. In the previous section, we saw that the magnitude of both these velocities is minimal at the retraction rate at which the tangential foot speed is zero. Based on this we can conclude that swing-leg retraction can decrease impact losses and that the optimal retraction rate, for which the impact losses are minimal, is the retraction at which the tangential foot speed is zero.

C. Slipping

Slipping of the foot at touchdown is a common problem for running and hopping robots [2]. Slipping occurs at impact when the horizontal impact impulse is too high compared to

the vertical impact impulse. The horizontal impulse caused by the foot mass $I_{x,foot}$ is given by,

$$I_{x,foot} = m_{foot} v_x. \tag{12}$$

The horizontal impulse caused by the leg inertia $I_{x,leg}$ is function of the leg mass m and the leg inertia J_{leg},

$$I_{x,leg} = \frac{J_{leg} m}{m L_0^2 + J_{leg}} sin(\alpha_0) v_t. \tag{13}$$

If the horizontal impulse is zero then the robot will not slip, no matter what the vertical impulse is. The horizontal impulse caused by the foot mass is zero if the horizontal foot speed v_x is zero, while the horizontal impulse caused by the leg inertia is zero for zero tangential foot speed v_t. The combined horizontal impulse $I_{x,foot} + I_{x,leg}$ is zero for a retraction rate between the retraction rate of zero tangential foot speed and the retraction rate of zero horizontal foot speed. The exact optimal retraction rate depends on the foot mass and leg inertia.

D. Impact forces

High impact forces can cause damage to a running robot. Swing-leg retraction might decrease these damaging impact forces. We assume that the impact is an instantaneous collision, which does not have finite impact forces. Therefore, we look instead at the impact impulses and assume that these are proportional to the impact forces if the collision were to take place over non-zero time. The impact impulse in the axial direction I_a is only caused by the unsprung foot mass and is given by,

$$I_a = m_{foot} v_a. \tag{14}$$

The impact impulse in the tangential direction I_t is more complex as it is caused by the combination of the impact of the foot and the impact of the leg,

$$I_t = \left[\frac{J_{leg} m}{m L_0^2 + J_{leg}} + m_{foot} \right] v_t. \tag{15}$$

Swing-leg retraction only affects the impact impulse in the tangential direction, as the leg retraction does not influence the axial foot speed. The absolute impulse $\sqrt{I_a^2 + I_T^2}$ is minimal as the impulse in the tangential direction is zero, which is at the retraction rate at which the tangential foot speed is zero. This optimal retraction for minimal impact impulse is the same as the optimal retraction rate for minimal impact losses.

V. DISCUSSION

A. Optimal retraction rates

In the previous two sections, we have shown that swing-leg retraction can improve the disturbance rejection as well as decrease the impact losses, the likelihood of slipping, and impact forces. However, the optimal retraction rates for these benefits can be different. Figure 7 shows the optimal retraction rate as a function of horizontal velocity. For low horizontal velocities, around 3 m/s, the optimal retraction rates are almost equal. But at higher horizontal velocities

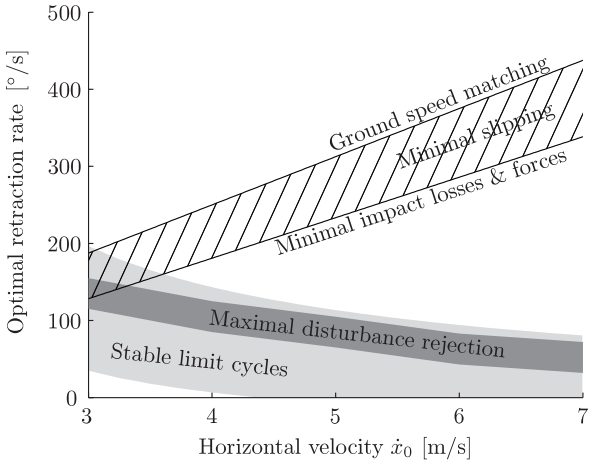

Fig. 7. The optimal retraction rates for maximal disturbance rejection (dark gray area), for minimal impact losses and forces (solid line) and for minimal slipping (striped area). The light gray area indicates which retraction rates result in stable limit cycles.

the optimal retraction rates diverge. The optimal retraction rate for the disturbance rejection decreases for increasing horizontal velocity, whereas the optimal retraction rate for impact losses, slipping, and impact forces increases with increasing horizontal velocity. At higher horizontal velocities, the optimal retraction rate for impact losses, slipping, and impact forces is so high that this retraction rate would destabilize the model.

B. Implications for running robots

The results of this paper are applicable to running robots with a wide variety of control schemes. For running robots that use swing-leg retraction as a complete angle-of-attack controller, the results indicate that only the range of stable retraction rates can be used. For retraction rates outside this range, the robot will fall in response to the smallest disturbance. Within the small range of retraction rates, the retraction rate is, in general, a tradeoff between maximal disturbance rejection and minimal impact losses, slipping likelihood and impact forces.

However, it is also possible to implement swing-leg retraction in conjunction with other angle-of-attack controllers. For example, Raibert's foot placement strategy could be used to determine the nominal angle-of-attack based on known disturbances, while swing-leg retraction can be used to rotate the leg backwards about this position to reduce the effect of small unknown disturbances and measurement errors. These combined controllers can be used to improve the disturbance rejection even more. The combined controllers can also be used in a different way, where swing-leg retraction is used to reduce the impact losses and forces and the likelihood of slipping, while the other controller provides the stability. For this last method, high retraction rates can be used that reduce impact losses and forces and likelihood of slipping to their minimum, because the other controller can compensate for the instability caused by these high retraction rates.

C. Implementation of swing-leg retraction on running robots

To implement swing-leg retraction on a running robot, the robot needs to be able to measure three quantities during the flight phase: the absolute angle, the angular rate of the leg, and the apex time. The apex time and the leg angle are needed to start the retraction at the correct moment with the desired leg angle. The angular rate is needed to control the leg to the desired retraction rate. The absolute angle and angular rate of the leg are often measured using a combination of accelerometers and gyroscopes. To determine the time of apex is more complicated. It can be done by integrating the vertical acceleration starting from liftoff or by using a contactless distances sensor, for example a laser rangefinder. Another option, for which the apex time is not needed, is to start the timer for the retraction on an easier to measure event, like the liftoff. However, starting the timer on a different event might have negative consequences on the stability and disturbance rejection. Preliminary results showed that starting the timer at liftoff significantly reduced stability, but more research is needed on this topic.

VI. CONCLUSIONS

In this paper, we presented a simulation study on swing-leg retraction. We showed how the benefits of swing-leg retraction depend on the retraction rate. Based on these results we conclude that:

- Swing-leg retraction can improve the disturbance rejection and reduce impact energy loss, likelihood of slipping, and impact forces.
- The optimal swing-leg retraction rate for maximal disturbance rejection only depends on the horizontal velocity and does not depend on any other parameter, like leg stiffness, angle-of-attack and apex height.
- The swing-leg retraction rates for optimal stability and maximal disturbance rejection decrease with increasing horizontal velocity.
- The swing-leg retraction rates for minimal impact energy loss, slipping likelihood, and damaging forces increases with increasing horizontal velocity
- For moderate and high running speeds, there is an inherent tradeoff between improving disturbance rejection and decreasing impact losses, impact forces, and slipping likelihood. This tradeoff becomes more severe as horizontal velocity increases.

REFERENCES

[1] R. Playter, M. Buehler, and M. Raibert, "BigDog," in *Proceedings of SPIE*, vol. 6230, 2006, p. 62302O.

[2] M. Raibert, *Legged robots that balance*. MIT press Cambridge, MA, 1986.

[3] R. Blickhan, "The spring-mass model for running and hopping," *Journal of Biomechanics*, vol. 22, no. 11-12, pp. 1217–1227, 1989.

[4] S. Kim, J. Clark, and M. Cutkosky, "isprawl: Design and tuning for high-speed autonomous open-loop running," *The International Journal of Robotics Research*, vol. 25, no. 9, p. 903, 2006.

[5] T. McGeer, "Passive bipedal running," *Proceedings of the Royal Society of London. Series B, Biological Sciences*, vol. 240, no. 1297, pp. 107–134, 1990.

[6] Y. Blum, S. Lipfert, J. Rummel, and A. Seyfarth, "Swing leg control in human running," *Bioinspiration & Biomimetics*, vol. 5, p. 026006, 2010.

[7] A. Seyfarth, H. Geyer, and H. Herr, "Swing-leg retraction: a simple control model for stable running," *Journal of Experimental Biology*, vol. 206, no. 15, p. 2547, 2003.

[8] M. Wisse, C. Atkeson, and D. Kloimwieder, "Swing leg retraction helps biped walking stability," dec. 2005, pp. 295 –300.

[9] D. G. E. Hobbelen and M. Wisse, "Swing leg retraction for limit cycle walkers improves disturbance rejection," *IEEE Transactions on Robotics*, vol. 24, no. 2, pp. 377–389, 4 2008.

[10] M. Daley and J. Usherwood, "Two explanations for the compliant running paradox: reduced work of bouncing viscera and increased stability in uneven terrain," *Biology Letters*, vol. 6, no. 3, p. 418, 2010.

[11] W. Schwind and D. Koditschek, "Characterization of monoped equilibrium gaits," in *IEEE International Conference on Robotics and Automation*, 1997, pp. 1986–1992.

[12] A. Seyfarth, H. Geyer, M. Gnther, and R. Blickhan, "A movement criterion for running," *Journal of Biomechanics*, vol. 35, no. 5, pp. 649 – 655, 2002.

[13] D. G. E. Hobbelen and M. Wisse, "A disturbance rejection measure for limit cycle walkers: the Gait Sensitivity Norm," *IEEE Transactions on Robotics*, vol. 23, no. 6, pp. 1213–1224, 2007.